Hutchings, A.M., and Turchyn, A.V., 2021, A quantification of the effect of diagenesis on the paleoredox record in mid-Proterozoic sedimentary rocks: Geology, v. 49, https://doi.org/10.1130/G48774.1

Supplementary information

Section 1: Model details

The dataset used for this model was compiled and published by Sperling et al. (2015). We highlight the role of the total iron content of the sedimentary rock on the resulting iron speciation data with regards to the diagenetic effect of sulfidisation of iron minerals.

The total iron contained in the sediment (Fe_T) plays a critical role in the behaviour of the sediment during early diagenesis and thus its potential trajectory in an iron speciation cross plot. First, the Fe_T is the denominator in the Fe_{HR}/Fe_T ratio. We propose that at high Fe_T, the existing data suggests there is a maximum Fe_{HR}/Fe_T that can be found in sediment deposited in an anoxic water column. In other words, there is a limit as to how much Fe_{HR}—as a fraction of the total iron—can be found in sediment deposited under an anoxic, non-sulfidic, water column. To test this, we sort the extensive dataset compiled by Sperling et al. (2015) data into three categories based on total iron content: 0–2.5%, 2.5–5% and, greater than 5% total iron. For samples where $Fe_{PY}/Fe_{HR}<0.1$ (crosses on **Figures 2A,C,E, main text**)— rocks that have been exposed to negligible dissolved sulfide because they contain no pyrite—the mean Fe_{HR}/Fe_T (filled squares) and the mean+2SD (filled circles) is significantly different for samples with less than 2.5wt% FeT compared to samples with more than 2.5wt% FeT. The presence of euxinia in the water column causes the formation of Fe-sulfide minerals, increasing the efficacy of Fe_{HR} accumulation, allowing for samples with a higher Fe_{HR}/Fe_T (Lyons and Severmann, 2006). We note that there are exceptional environments where this is not the case, namely banded iron formations close to hydrothermal vents or in salt marsh/coastal lagoons (Neumann et al., 2005; Bekker et al., 2010).

Theoretically, diagenesis could shift a sample with an Fe_{PY}/Fe_{HR} value of zero close to a value of one if dissolved sulfide reacts with all available highly-reactive iron, converting it to iron sulfide minerals. As Fe_{PY} is one component of the Fe_{HR} pool, this diagenetic exchange of a 'generic' highly-reactive iron mineral for pyrite would not shift the Fe_{HR}/Fe_T (Raiswell et al., 2018). For a given Fe_{HR}/Fe_T deposited at the sediment water interface, a vertical line can be drawn upwards (reflecting changes in Fe_{PY}/Fe_{HR}) which reflects this conversion of highly-reactive iron minerals to pyrite. There may be some potential decrease in Fe_{HR}/Fe_T if iron minerals age to become more crystalline with time (Cornell and Schwertmann, 2003), thus decreasing the numerator, but we cannot see an environmentally-plausible method for the Fe_{HR}/Fe_T to shift towards the right post-depositionally other than the longer term conversion of unreactive iron to pyrite (thus increasing Fe_{PY}). We would argue that the timescale for this would be larger than the timescale of the diagenetic model runs we use (Raiswell and Canfield, 1996).

A more realistic framework than this Fe_{HR}/Fe_T threshold is one which considers the effect of time, sulfide-input rate and total iron content of the sediment. We use a simple calculation to demonstrate the effect of diagenetic sulfidisation, where a constant concentration of sulfide is introduced to sediment (Eq. 1 – main text). The amount of diagenetically produced $Fe_{HR \rightarrow PY}$ is a function of Fe_{HR}, the amount of pyrite which already exists in the sediment before diagenetic reactions occur ($Fe_{PY(ND)}$), the amount of dissolved sulfide introduced to the system [HS] and, the amount of time (t) that dissolved sulfide is introduced. Two moles of dissolved sulfide are necessary to convert one mole of iron to form pyrite, hence the division of the [HS] by 2 in the equation. In modern sediments, where Fe hosted in AVS may be more common, this division may require adjustment (Raiswell et al., 2018). For simplicity, we use fluxes per cm^{-3} of sediment using a marine sediment density of 1.7 g cm^{-3} (**Table S1**).

The dissolved sulfide is assumed to react and convert all Fe_{HR} to Fe_{PY} and thus the kinetics of individual reactions are not included. Given that dissolved sulfide will eventually react with highly-reactive iron minerals before being transported by diffusion, this is a fair assumption given the long timescales (the model is run for 1000+ years) (Raiswell and Canfield, 1996). For shorter time scales, this may not be as applicable, and kinetics of the reaction, as well as sediment mineralogy, should be included. We use a 200 pMol cm^3 day^{-1} flux in Figure 2 in accordance with estimates from the Black Sea (corresponding to porewater sulfide concentrations of 1.5 mM), though site specific rates would be more applicable (Egger et al., 2016). We chose the Black Sea for two reasons: (1) it has a known sulfate reduction zone with well quantified diagenetic reactions and (2) the Black Sea has a lower sulfate concentration than other marine settings due to the freshwater input into the sea which better reflects conditions in low sulfate oceans. We note that sulfide input rate will be heterogeneous over a sediment profile (as sediment is buried away from sulfate reduction zones or zones of AOM); a reactive transport model would obviously provide a more accurate constraint for this but would require detailed knowledge of an environment. **Figure S2** shows how variations in timing and the concentration of dissolved sulfide influence the model run.

Parameter (units)	**Figure 2A**	**Figure 2B**	**Figure 2C**
FeT (wt%)	2.5	5.0	10
Marine sediment density (g cm^{-3})	1.7	1.7	1.7
FeT (mMol g^{-1})	0.447	0.895	1.791
FeT (mMol cm^{-3})	0.761	1.522	3.044
Sulfide input (mMol cm^{-3} day^{-1})[A]	2×10^{-7}	2×10^{-7}	2×10^{-7}

Table S1 – List of parameters included in the model with unit conversions. ^Sulfide input rate is taken from diagenetic modelling in Egger et al., (2016).

We show the expected threshold lines for varying lengths of simulation time (the amount of time dissolved sulfide is introduced to the porewater). Longer simulation times than run for **Figure 2** (main text) would continue to trend towards a vertical line. There would be a point, depending on the sedimentation rate and whether a sedimentary column was advective or diffusive, where the sediment would no longer be in contact with sulfide, and this would be considered the preserved signal in the sedimentary rock. We use 30 kyrs is used as a first approximation for the scale of diagenesis, which is in accordance with modern sedimentary environments on continental shelves, where we argue this effect would be most prevalent (Egger et al., 2016; Liu et al., 2020).

Section 2: Estimates of the extent of this effect using Sperling et al. (2015) dataset

We estimate how many samples of the Sperling et al. (2015) dataset which were defined as euxinic in that study could be explained by diagenetic effects. We test differences in the amount of sulfide (either 100 or 200 pMol cm^{-3} day^{-1}), differences in the starting value of Fe_{PY} (whether the samples begin at Fe_{PY}/Fe_{HR} = 0 or 0.1) and variations in the total iron used for samples. The results of this are shown in **Table S2**.

Model Run / **Model conditions**	**1**	**2**	**3**	**4**	**5**	**6**	**7**	**8**
Time (years)	30000	30000	30000	30000	30000	30000	30000	30000
Initial Fe_{PY}/Fe_{HR}	0	0	0	0	0.1	0.1	0.1	0.1
Sulfide addition (pMol/cm^3/day)	200	200	100	100	200	200	100	100
Total iron (High or Low)	High	Low	High	Low	High	Low	High	Low
Fe_T (Wt%) fraction	**Percentage of samples explained by diagenetic overprinting (%)**							
<2.5%	100	100	73	100	100	100	84	100
2.5-5%	87	100	9	87	94	100	26	94
>5%	14	79	0	15	24	92	0	24
Total	**75**	**95**	**28**	**75**	**80**	**98**	**40**	**80**

Table S2 – *Estimations of the proportion of samples originally identified as 'euxinic' in Sperling et al. (2015) which may be explained by diagenetic effects alone. We vary the initial Fe_{PY}/Fe_{HR} between 0 and 0.1 which should reflect the variation in samples on deposition at the sediment-water interface in a ferruginous/oxic water column (these samples initially have no pyrite so have been exposed to negligible dissolved sulfide in their history). We tested the effect of sulfide addition at 100 and 200 pMol/cm^3/day based on estimates in Egger et al. (2016)(Egger et al., 2016) . We tested the effect of total iron by running the models at the lower and higher estimates of Fe_T in each range: Low* *corresponds to 0.1, 2.5 and 5 wt% iron from the <2.5%, 2.5-5% and >5% fractions respectively. High corresponds to 2.5, 5 and 10 wt% iron from the <2.5%, 2.5-5% and >5% fractions respectively. We ran eight model simulations with each combination of these. For a graphical representation of how samples were interpreted, see Figure S3. Note that these estimates include modern samples.*

Using variations in our inputs, the maximum proportion of samples which can be explained by solely diagenetic processes is 98%. This occurs when all samples initially contain a Fe_{PY}/Fe_{HR} of 0.1 at deposition, the total iron content is at the lowest boundary for each fraction (ie. 0.1 wt%, 2.5 wt% and 5 wt%) and dissolved sulfide is supplied at the higher rate of 200 pMol/cm^3/day. The <2.5 wt% iron fraction can be completely explained by diagenesis in six of the eight model runs implying how susceptible samples with low total iron are to this overprinting effect.

We conclude that the most reasonable range is between 75 and 80% of samples previously identified as euxinic which could be explained solely by post-depositional diagenesis. As many of the inputs have similar effects on the results (i.e. a halving of sulfide production rate has the same effect as doubling the total iron), this range of estimates is more likely to correspond to the majority of samples if the sample set has a normal Gaussian distribution. We did not test the effect of time, though this can be logically understood as a longer diagenetic effect will result in more samples being diagenetically overprinted.

To ascertain whether samples in certain time periods may be more or less susceptible to this diagenetic effect, we split the revised estimates by age bins used in Sperling et al. (2015) (**Figure 3**). We use the conditions in model run 4 to split samples into a refined true euxinic vs diagenetically altered samples (**Table S2**). We find that roughly 7% of the 2300–1100Ma samples from the Sperling et al. (2015) dataset show true euxinia. This is a large decrease from the original estimated proportion of euxinic samples (25%) but is more in line with independent estimates from marine carbonates (Gilleaudeau et al., 2019). The limited number of samples from 1000–365Ma makes any interpretations tricky. All modern samples can be explained by solely diagenesis, decreasing the extent of true euxinic samples from 25% to 0%. This is quite notable considering that the Raiswell and Canfield, (1998) dataset was used as the modern component of the Sperling et al. (2015) dataset; this study specifically targeted sites with anoxic bottom water and so is heavily biased towards anoxic settings. The low iron content in modern sediments combined with high sulfate concentrations means that diagenetic overprinting would be very common in modern sediments, though the oxic nature of the modern ocean prevents this from imparting a major bias in the record.

We acknowledge that certain samples may well have conditions that lie outside the model inputs we have described here. The fact that roughly three quarters of iron-speciation samples can be reasonably explained by diagenesis however is striking. It likely does not detract from the conclusions of the work of Sperling et al. (2015) as relative proportions would still likely show the interpreted change in euxinia with time, though it does suggest that the total amount of euxinia was less through Earth history.

Section 3: Evaluating the diagenetic effect on the Liu et al. (2020) dataset

To test the applicability of these interpretations to modern sediments, we trial it on the recently published iron speciation dataset from the Bornholm Basin (Liu et al., 2020). The authors of this paper presented iron speciation measurements which would canonically be interpreted to have been deposited under euxinic conditions, despite the lack of a euxinic water column. This therefore seemed the ideal dataset to check for early sediment diagenesis.

Using their published sedimentation rates, we first plot a composite figure of the Fe_{Py}/Fe_{HR} with age (**Figure S1**). Sediments recently deposited have an Fe_{Py}/Fe_{HR} of 0.2–0.6 which rapidly increases (within 1500 years) to 0.8–0.9. This represents burial of iron minerals (deposited at the sediment-water interface) into the sulfate reduction zone where they are exposed to dissolved sulfide and the iron speciation signature is altered. A similar effect is also observed at Long Island Sound, USA in the study conducted by (Hardisty et al., 2018). For sediments that are around 8000 years old, this effect is not observed. This represents the transition from lacustrine clays deposited at the last glacial maximum into the current organic-rich environment. Notably, one sample from the lacustrine clay lies between the higher Fe_{Py}/Fe_{HR} and the post 8000-year Fe_{Py}/Fe_{HR} values; this may represent downward migration of the dissolved sulfide produced in the overlying organic-rich sediment.

We test the iron speciation data from three cores in the Liu et al. (2020) study. The sedimentation rate at this site is quite high relative to that modelled in **Figure 2** and thus should be treated with some caution. We use the highest Fe_T from each sediment core to establish the minimum effect of diagenesis over time (our model shows that lower Fe_T would be more easily overprinted). We also neglect the role of Fe associated with AVS in these modern sediments, which would potentially increase the role of the diagenetic overprinting effect. If we use the minimum Fe_T measured, all samples lie beneath the modelled zone that can be explained by diagenetic overprinting. The modelled lines in **Figure S4** represent the time for the sediment to have been buried if sedimentation rate is constant with time. This is likely an underestimation of the true time as sedimentation rates may vary. Based on the roughly 150% higher dissolved sulfide concentrations present in the Bornholm Basin compared to the Black sea, we simulate a 300 pMol/cm^3/day sulfide flux. Despite these conservative inputs, the Fe_{Py}/Fe_{HR} ratio of only 9 samples are not explained by diagenesis alone. By lowering the Fe_T value even modestly, all samples can be explained readily.

We suggest this lends faith to our model as a test for diagenetic effect. Had the Bornholm Basin samples had a high Fe_{HR}/Fe_T ratio and high Fe_T contents, we would not be able to explain this effect through diagenesis. We find our model accurately predicts the conclusions of the authors of the study.

Supplementary figure captions

Figure S1 – *Sediment age plotted against (a) Fe_{PY}/Fe_{HR} and (b) Fe_{HR}/Fe_{T} ratios. Sediment age was calculated by multiplying sediment depth by the sedimentation rate given in Liu et al. (2020). Sediments are deposited at sediment-water interface with a low (<0.4) Fe_{PY}/Fe_{HR} ratio, but upon burial into the sulfide production zone, become diagenetically altered to high >0.8 Fe_{PY}/Fe_{HR} ratios.*

Figure S2: *Estimate time taken for complete pyritization of the highly reactive iron pool in sediment (i.e. the time taken for Fe_{PY}/Fe_{HR} to increase from 0 to 1) based on total iron content in the sediment (1-10%). High and low sulfide fluxes correspond to 400 pMol cm^{-3} d^{-1} and 200 pMol cm^{-3} d^{-1} respectively. A higher Fe_{HR}/Fe_{T} ratio for the same Fe_{T} value means more of the iron is highly reactive, and thus susceptible to pyritization.*

Figure S3 – *Graphical representation of the selection criteria shown in Table 1 for Model Run 7. Dashed line represents the diagenetic model (**Figure 2, main text**) run for (A) 2.5% Fe_{T}, (B) 5% Fe_{T} and, (C) 10% Fe_{T}. Datapoints are the iron speciation datapoints from Sperling et al. (2015) for (A) >2.5% Fe_{T} samples, (B) 2.5% - 5% Fe_{T} samples and (C), >5% Fe_{T} samples. Samples highlighted in red lay in the euxinic portion of the classical speciation criteria and cannot be solely explained by diagenetic effects.*

Figure S4 – *Recently published data from the Bornholm Basin with our model plot on the iron-speciation framework using total iron and sedimentation rates from Liu et al., 2020 to assess the timing of the sediment overprinting. We use a starting Fe_{PY}/Fe_{HR} ratio of 0.2 as this appears to be the approximate value of sediment at the sediment-water interface (see Supplementary Figure 1). Note we use the maximum Fe_{T} for each sediment core thus representing the maximum resistance to the diagenetic effect. Red dashed line (Run for 1231 years, 0.2343 mMol/g Fe_{T}) represents simulated BB01 RL-4 core. Black dashed line (Run for 1132 years, 0.2365 mMol/g Fe_{T}) represents simulated BB02 RL-5 core. Blue dashed line (Run for 1378 years, 0.2390 mMol/g Fe_{T}) represents simulated BB05 RL-5 core. We use 300 pMol cm^{3} day^{-1} as the sulfide flux based on scaling the sulfide concentrations to the Black Sea estimates* (Egger et al., 2016).

References

Bekker, A., Slack, J.F., Planavsky, N., Krapez, B., Hofmann, A., Konhauser, K.O., and Rouxel, O.J., 2010, Iron Formation: The Sedimentary Product of a Complex Interplay among Mantle, Tectonic, Oceanic, and Biospheric Processes: Economic Geology, v. 105, p. 467–508, doi:10.2113/gsecongeo.105.3.467.

Cornell, R.M., and Schwertmann, H.C.U., 2003, The Iron Oxides: Structure, Properties, Reactions, Occurences and Uses, Second Edition:

Egger, M., Kraal, P., Jilbert, T., Sulu-Gambari, F., Sapart, C.J., Röckmann, T., and Slomp, C.P., 2016, Anaerobic oxidation of methane alters sediment records of sulfur, iron andphosphorus in the Black Sea: Biogeosciences, v. 13, p. 5333–5355, doi:10.5194/bg-13-5333-2016.

Gilleaudeau, G.J. et al., 2019, Uranium isotope evidence for limited euxinia in mid-Proterozoic oceans: Earth and Planetary Science Letters, v. 521, p. 150–157, doi:10.1016/j.epsl.2019.06.012.

Hardisty, D.S. et al., 2018, An evaluation of sedimentary molybdenum and iron as proxies for pore fluid paleoredox conditions: American Journal of Science, v. 318, p. 527–556.

Liu, J., Pellerin, A., Antler, G., Kasten, S., Findlay, Alyssa.J., Dohrmann, I., Roy, H., Turchyn, A.V., and Jørgensen, B.B., 2020, Early diagenesis of iron and sulfur in Bornholm Basin sediments: the role of near-surface pyrite formation: Geochimica et Cosmochimica Acta, v. 284, p. 43–60.

Lyons, T.W., and Severmann, S., 2006, A critical look at iron paleoredox proxies: New insights from modern euxinic marine basins: Geochimica et Cosmochimica Acta, v. 70, p. 5698–5722, doi:10.1016/j.gca.2006.08.021.

Neumann, T., Rausch, N., Leipe, T., Dellwig, O., Berner, Z., and Böttcher, M.E., 2005, Intense pyrite formation under low-sulfate conditions in the Achterwasser lagoon, SW Baltic Sea: Geochimica et Cosmochimica Acta, v. 69, p. 3619–3630, doi:10.1016/j.gca.2005.02.034.

Raiswell, R., and Canfield, D.E., 1996, Rates of reaction between silicate iron and dissolved sulfide in Peru Margin sediments: Geochimica et Cosmochimica Acta, v. 60, p. 2777–2787, doi:10.1016/0016-7037(96)00141-X.

Raiswell, R., Hardisty, D.S., Lyons, T.W., Canfield, D.E., Owens, J.D., Planavsky, N.J., Poulton, S.W., and Reinhard, C.T., 2018, The iron paleoredox proxies: A guide to the pitfalls, problems and proper practice: American Journal of Science, v. 318, p. 491–526.

Source code for 2.5wt% FeT input model (e.g. Figure 2A):

```
FeTLow = 0.447*1.7; %mMol/g times by the average marine density of 1.7
g/cm3
FeHRFeT = 1;%Threshold value dictated
HS = 200*1e-9*365; %unit conversion to mMol/cm3/year

%Time step creation
for t = 100:10000:30100 %Start at 100 years to simulate short term changes
%Create array for model input
for i = 1:100
    FeHRFeTInput(i) = FeHRFeT*0.01*i; %Step to dictate each FeHr/FeT value
(1-100)
end

%Function
Output=(FeHRFeTInput*FeTLow)-((HS/2)*t); %Times = ratio by total iron -
(sulfide*the time step)
%The output is the amount of iron left after converstion to pyrite.
```

```
for i = 1:100
    if Output(i) <= 0;
        Output(i) = 0;
    end
end

FePYFeHR = ((FeHRFeTInput*FeTLow)-Output)./(FeHRFeTInput*FeTLow); %The
FeHR/FeT ratio
plot(FeHRFeTInput,FePYFeHR,'--r','linewidth',2)
end
ylim([0 1])
xlim([0 1])
```

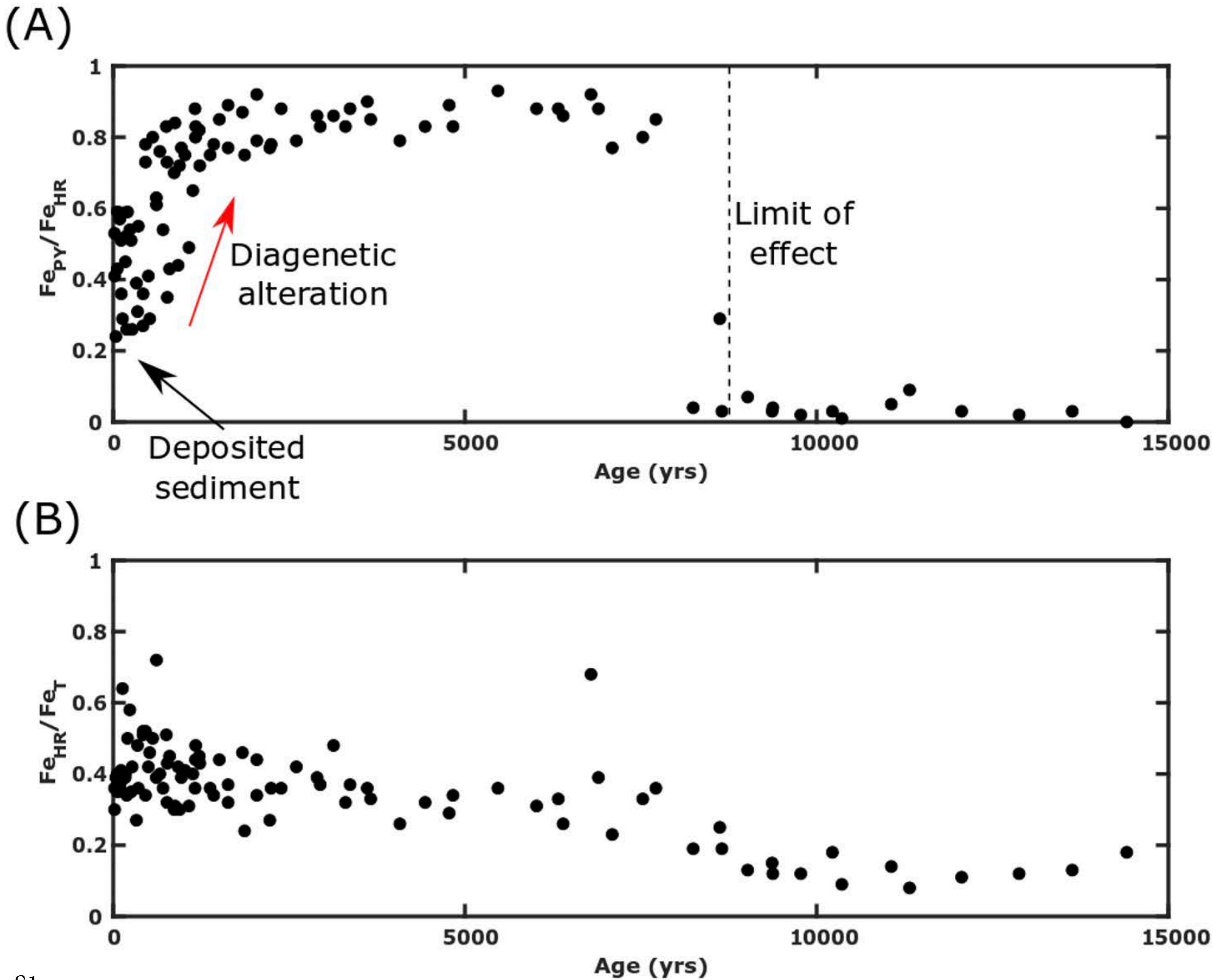
(A)
1
0.8
0.6
0.4
0.2
0
Fe$_{PY}$/Fe$_{HR}$
Diagenetic alteration
Limit of effect
Deposited sediment
0
5000
10000
15000
Age (yrs)
(B)
1
0.8
0.6
0.4
0.2
0
Fe$_{HR}$/Fe$_{T}$
0
5000
10000
15000
Age (yrs)

Fig. S1

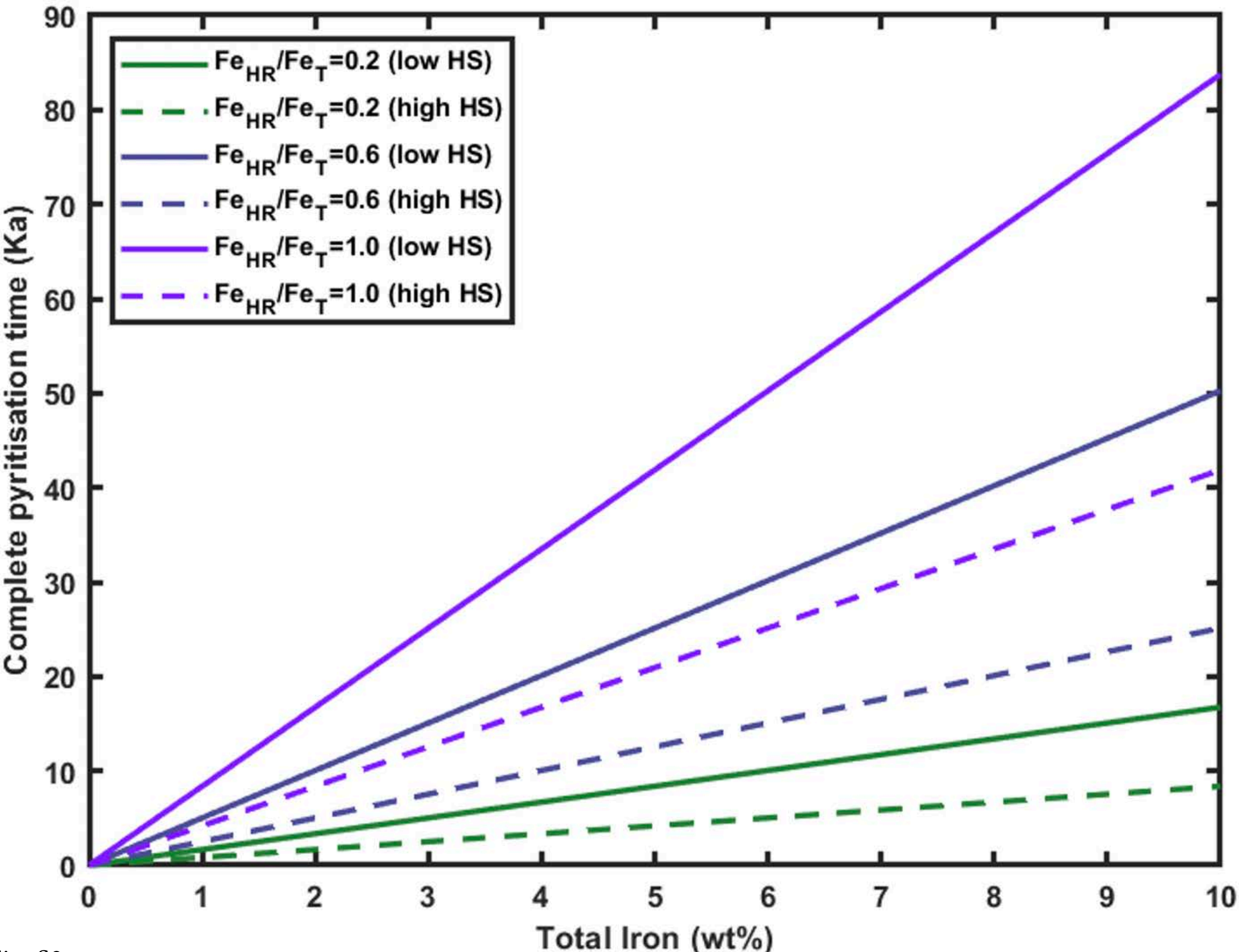

Fe_{HR}/Fe_T=0.2 (low HS)
Fe_{HR}/Fe_T=0.2 (high HS)
Fe_{HR}/Fe_T=0.6 (low HS)
Fe_{HR}/Fe_T=0.6 (high HS)
Fe_{HR}/Fe_T=1.0 (low HS)
Fe_{HR}/Fe_T=1.0 (high HS)
Complete pyritisation time (Ka)
0
10
20
30
40
50
60
70
80
90
0
1
2
3
4
5
6
7
8
9
10
Total Iron (wt%)

Fig. S2

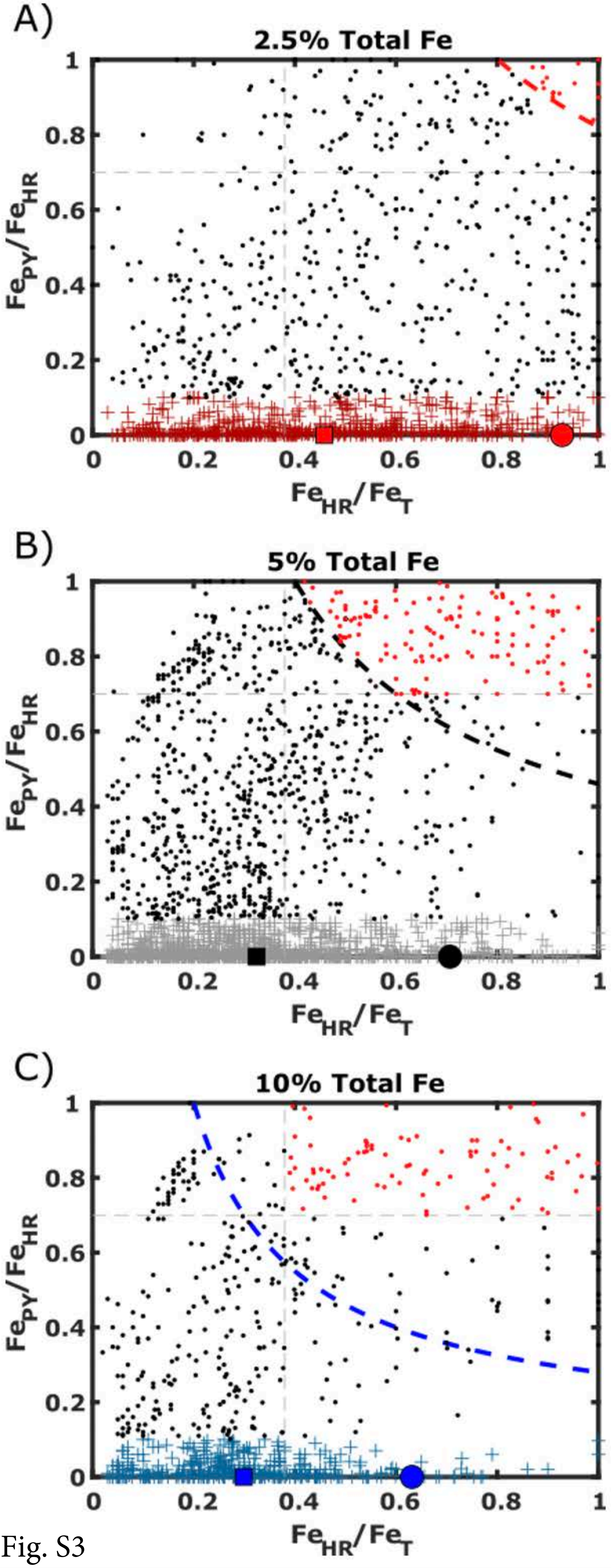

A)
2.5% Total Fe
B)
5% Total Fe
C)
10% Total Fe
Fe_{PY}/Fe_{HR}
Fe_{HR}/Fe_{T}
0
0.2
0.4
0.6
0.8
1

Fig. S3

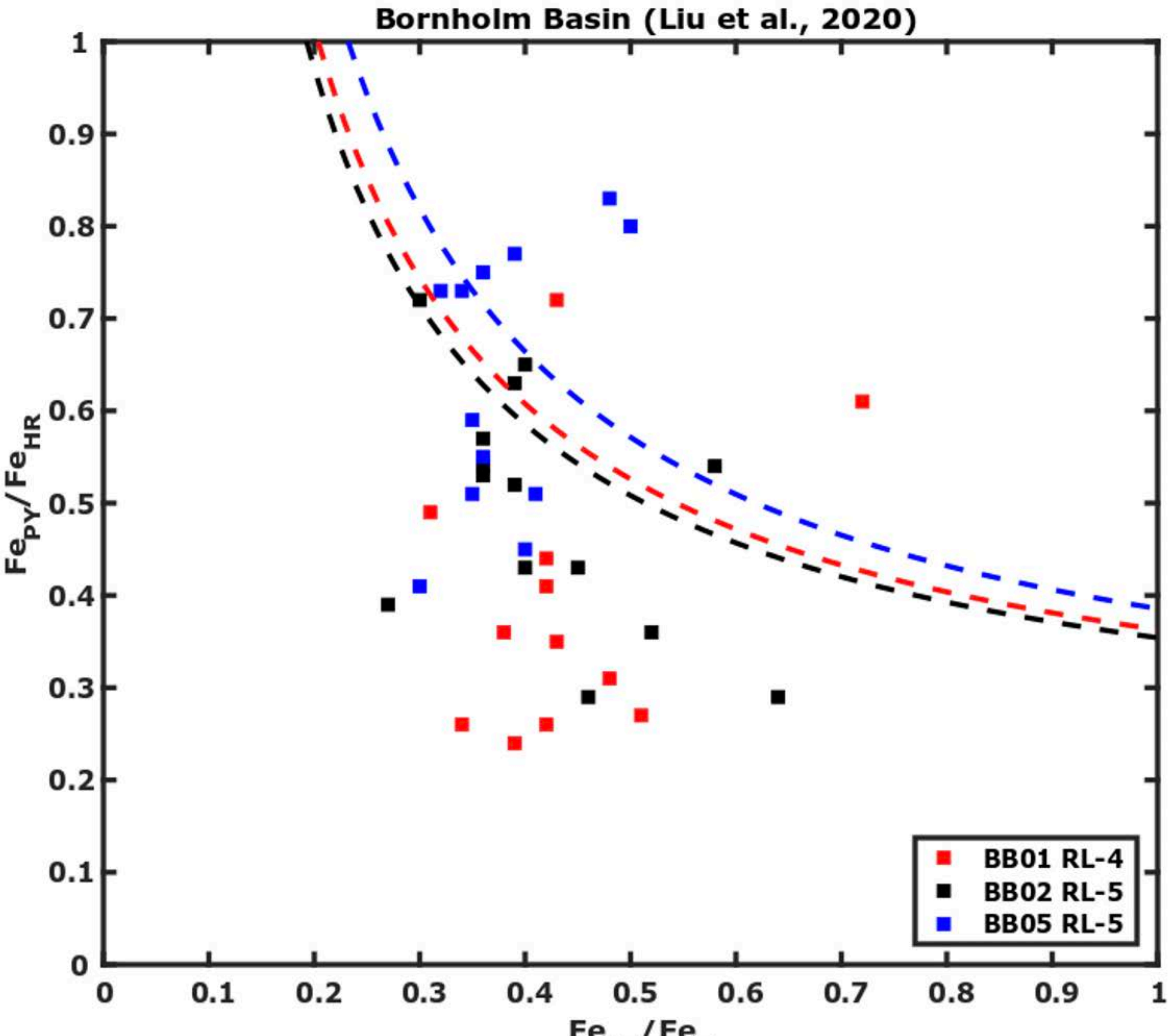

Bornholm Basin (Liu et al., 2020)
Fe_{PY}/Fe_{HR}
Fe_{HR}/Fe_{T}
0
0.1
0.2
0.3
0.4
0.5
0.6
0.7
0.8
0.9
1
BB01 RL-4
BB02 RL-5
BB05 RL-5

Fig. S4